## Appendix

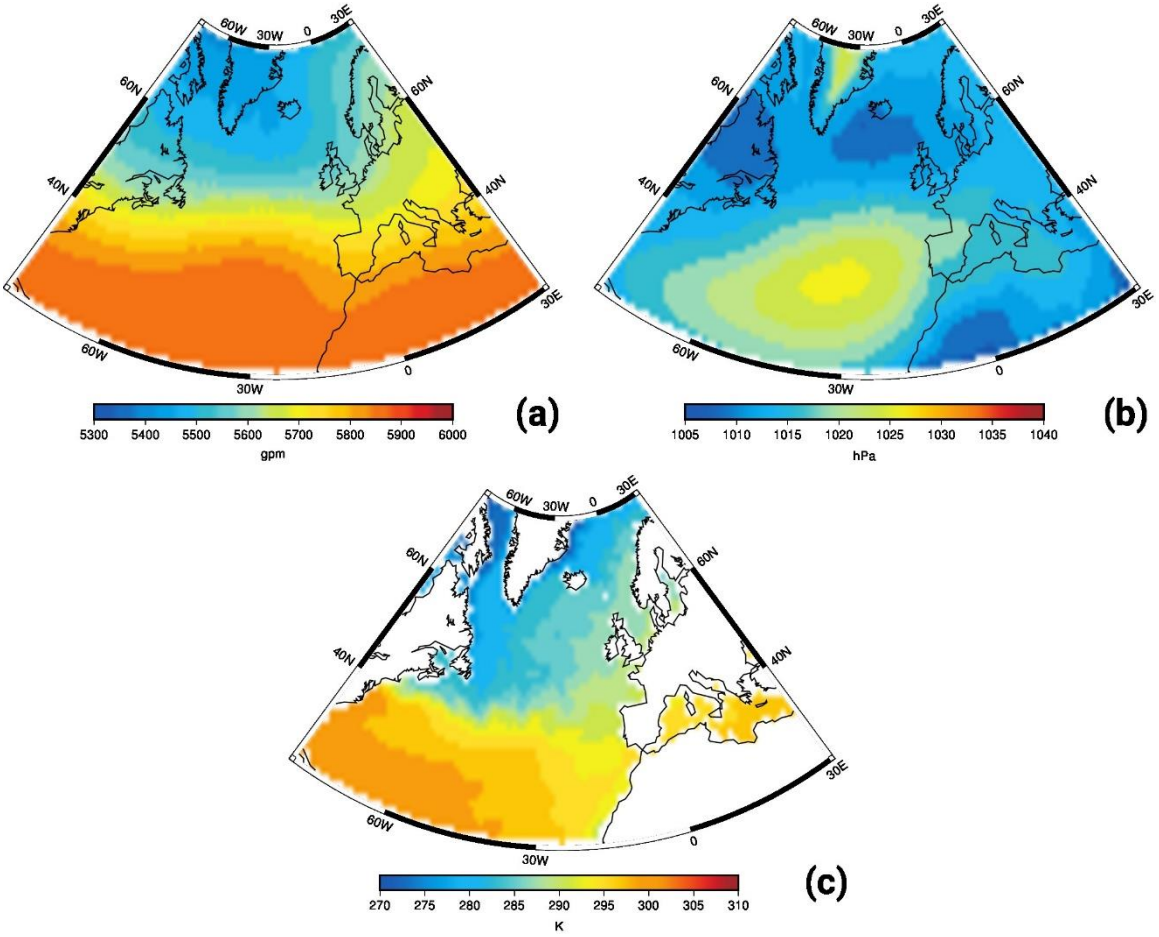


**Figure S1.** Mean summer values for (a) geo500 hPa, (b) SLP and (c) SST for the period 850–1849 AD and the realization R4 of the MPI-ESM model.

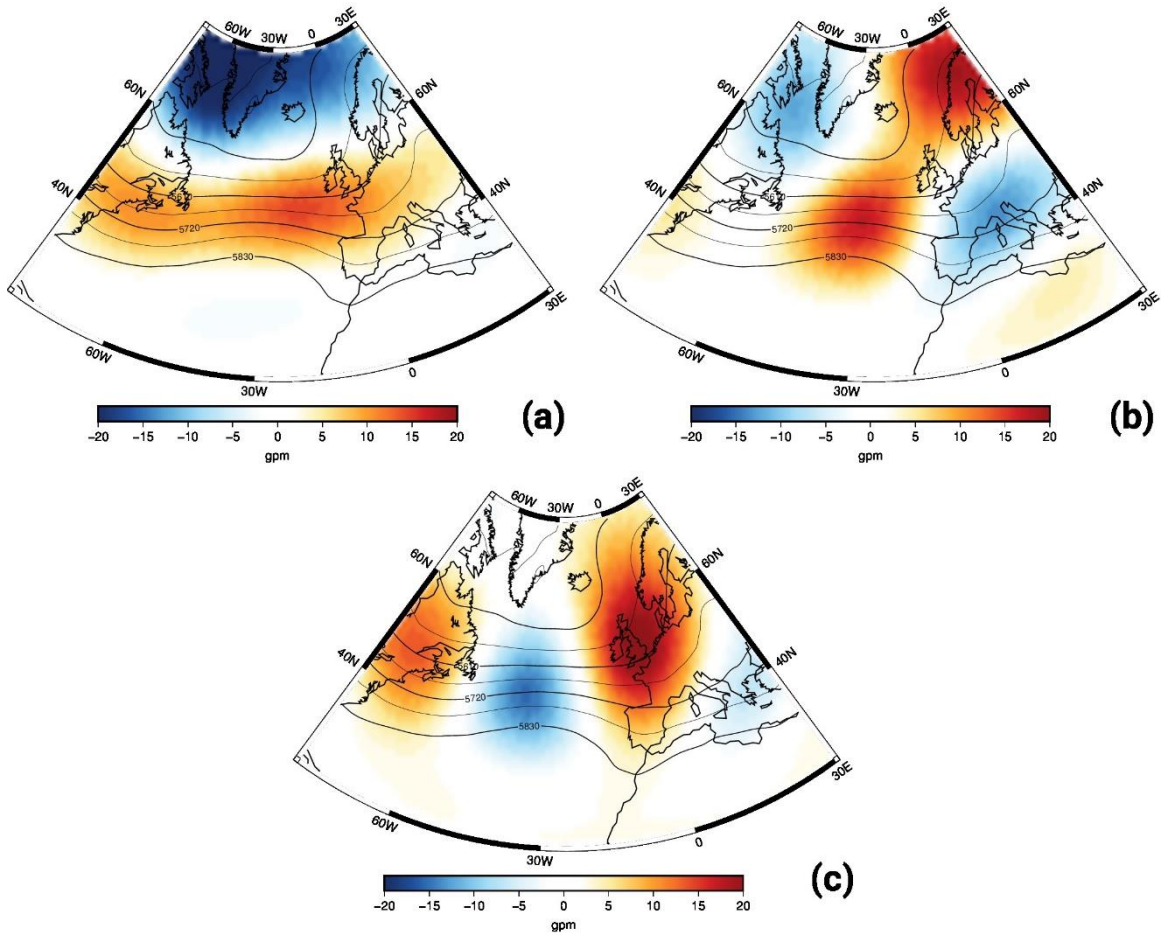


**Figure S2.** Summer EOFs of geo500 for the realization R4 of the MPI-ESM model, for the period 850–1849 AD. The first, second and third EOFs are given in (a) EOF1, (b) EOF2 and (c) EOF3, respectively.

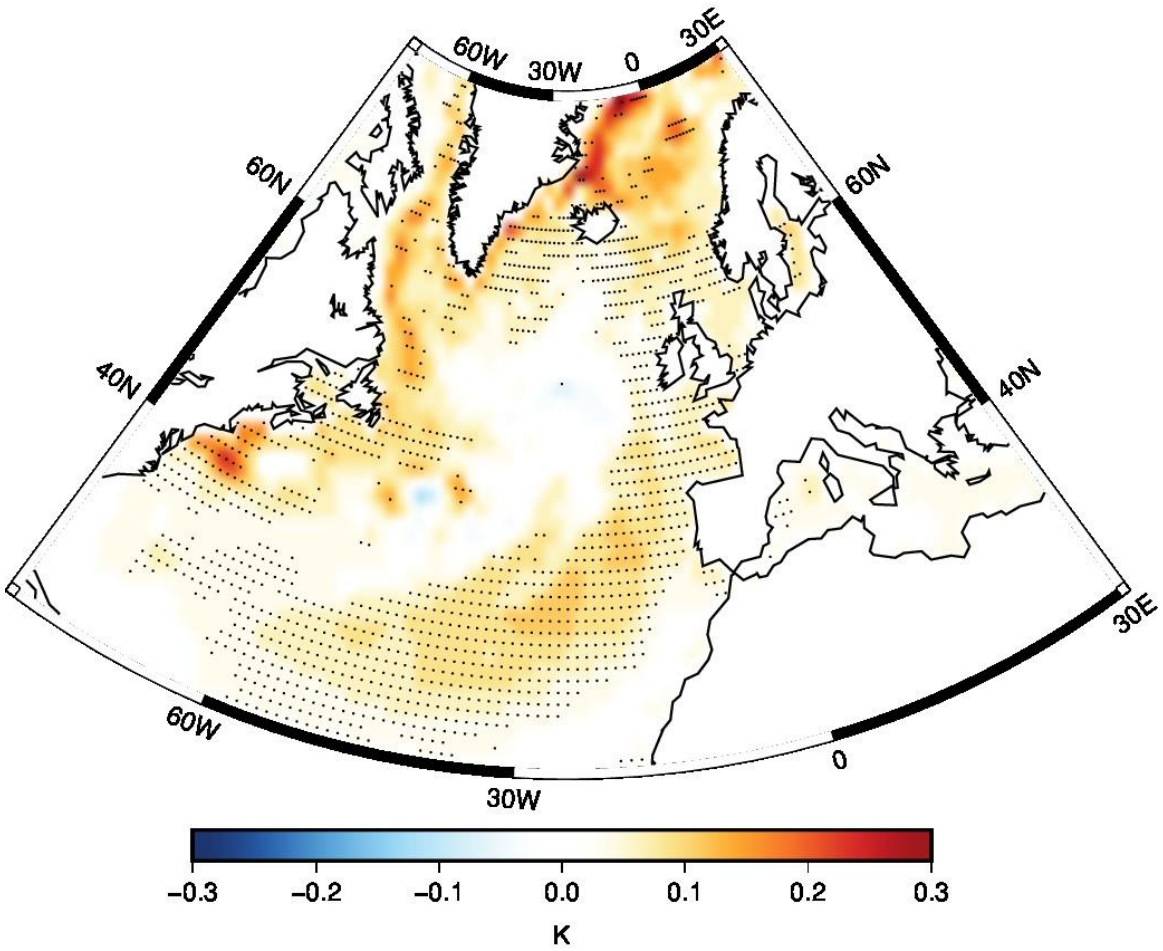


**Figure S3.** Regression of the TSI anomalies to the SST of the NA basin for the period 850–1849 AD and the realization R1 of the MPI-ESM model. The hatched areas indicate statistical significance at the 5% level taking into account the effect of serial correlation.

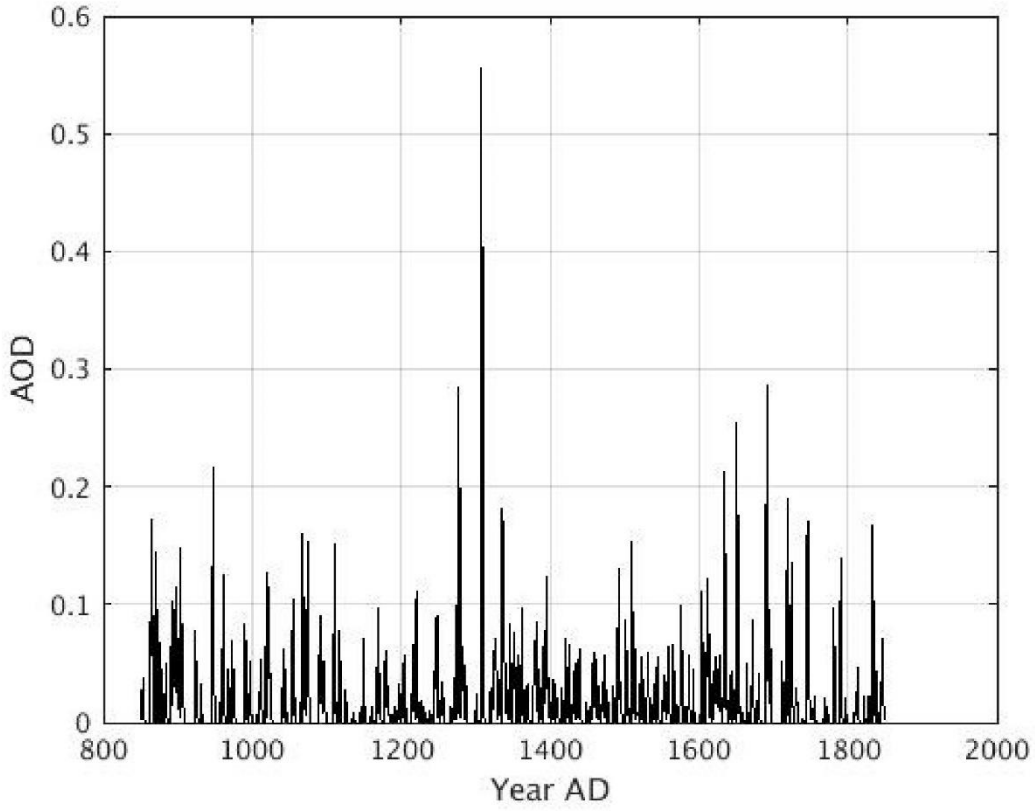


**Figure S4.** Aerosol Optical Depth due to volcanic aerosols, for the area 30°N–90°N and the period 850–1849 AD.

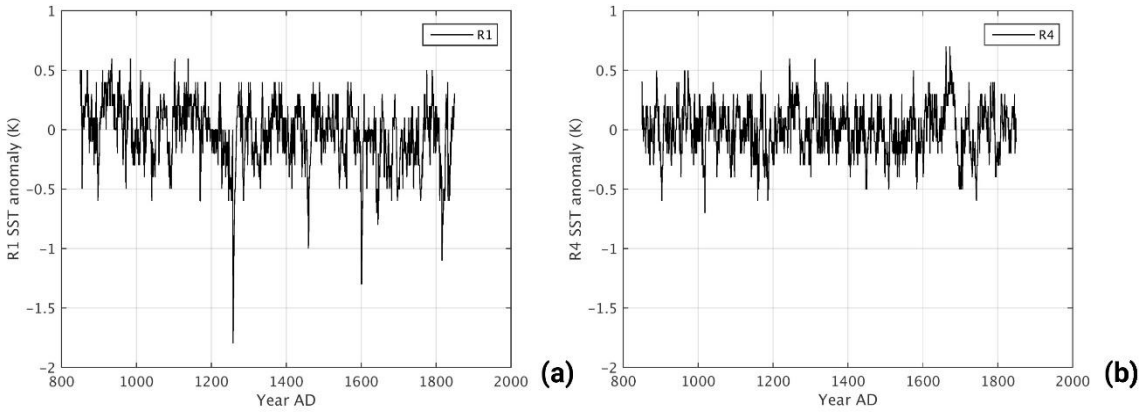


**Figure S5.** Detrended SST anomalies, averaged over the NA basin for the period 850–1849 AD and the realizations (a) R1 and (b) R4 of the MPI-ESM-P model.

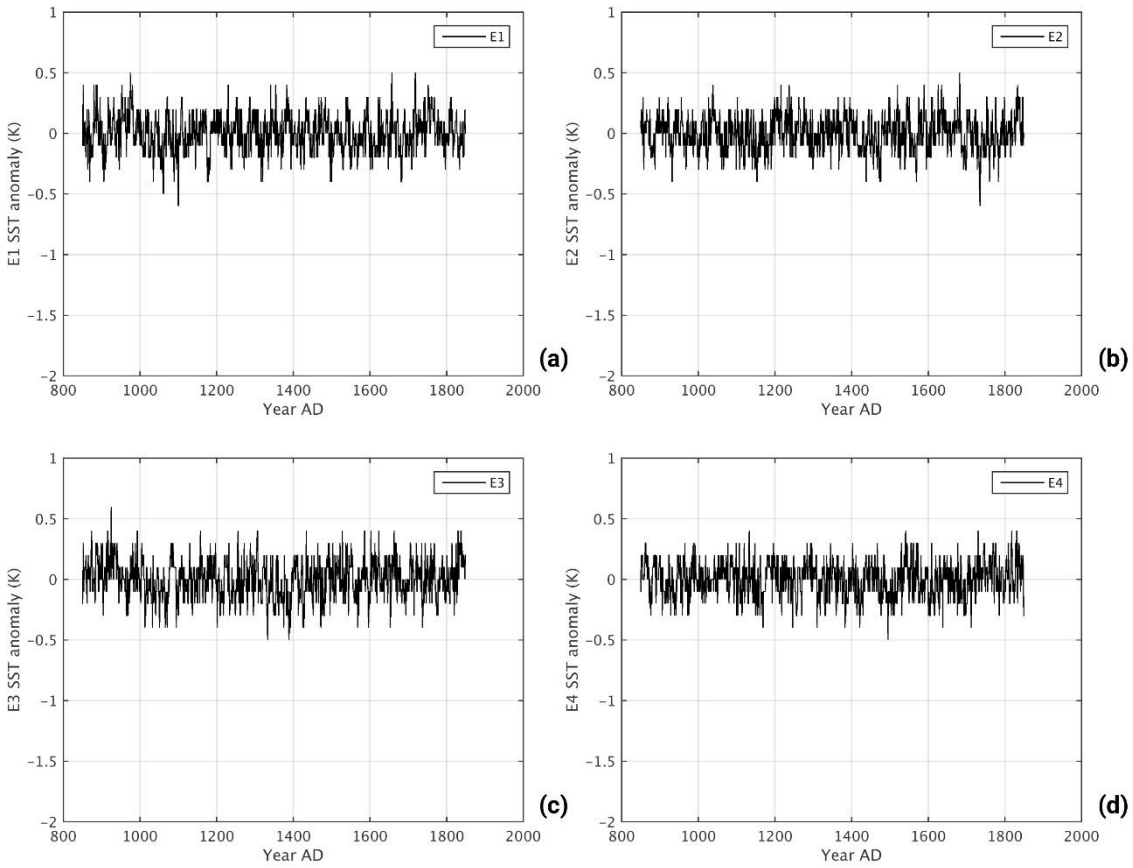


**Figure S6.** Detrended SST anomalies, averaged over the NA basin for the period 850–1849 AD and the realizations (a) E1, (b) E2, (c) E3 and (d) E4 of the CESM model.

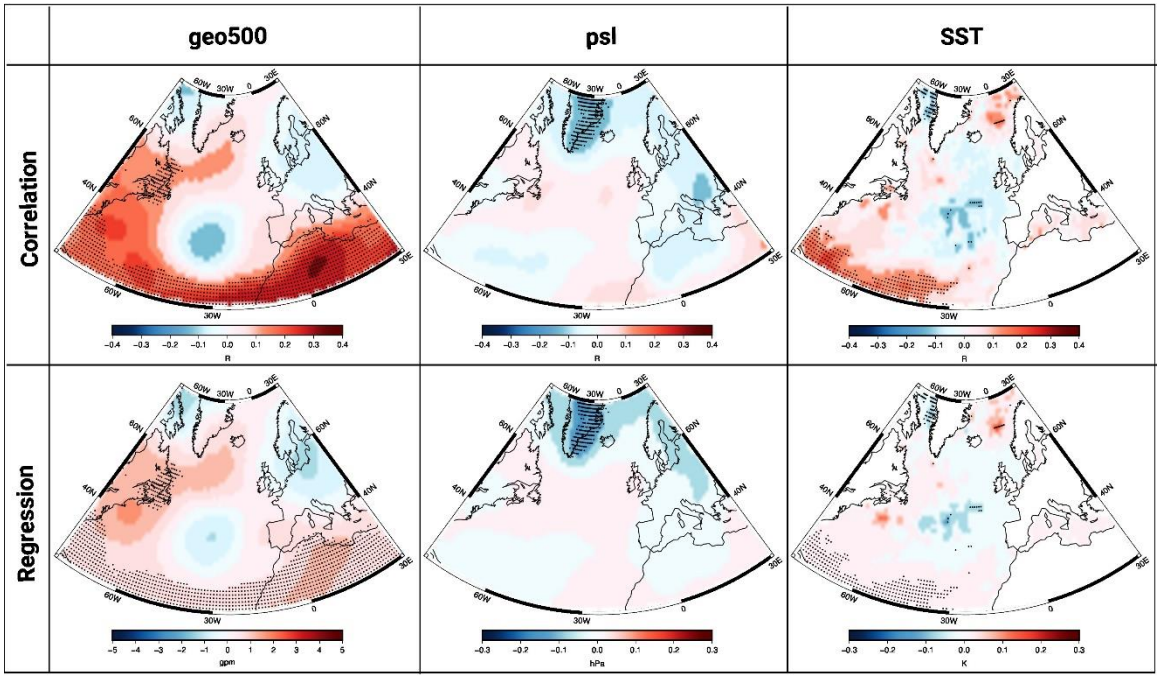


**Figure S7.** Spatial climatic response patterns of the North Atlantic geo500 (first column), SLP (second column) and SSTs (third column) due to TSI changes during the summer, as calculated with linear

methods for the period 850–1849 AD and for decadal time scales. The results regard the MPI-ESM model and are given for the pointwise correlation and regression of TSI with the climatic variables in rows one and two, respectively. The hatched areas indicate statistical significance at the 5% level taking into account the effect of serial correlation. In the case of the linear regression, the units refer to changes of 1 standard deviation.

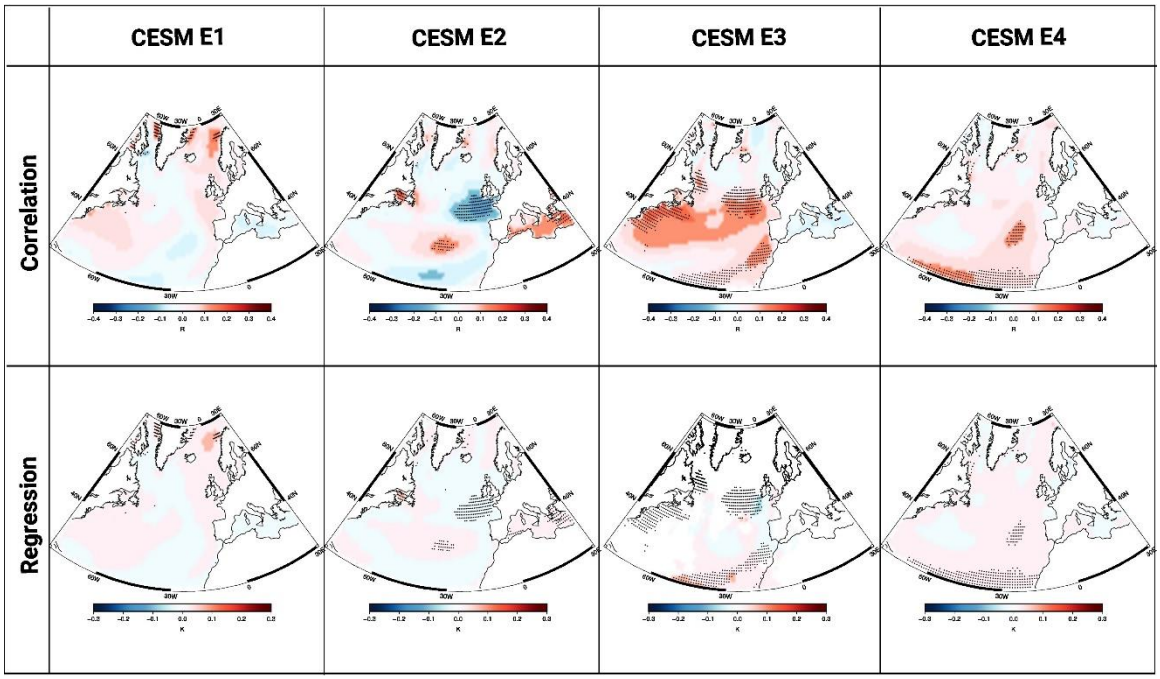


**Figure S8.** Spatial climatic response patterns of the North Atlantic SSTs due to TSI changes during the summer, as calculated with linear methods for the period 850–1849 AD and for decadal time scales. The spatial correlation between TSI and the NA SSTs is given in the first row. The second row contains the results of the regression of the TSI anomalies to the NA SSTs. In the case of the linear regression, the units refer to changes of 1 standard deviation. The results are given for the realizations E1, E2, E3 and E4 of the CESM model in the first, second, third and fourth column, respectively. The hatched areas indicate statistical significance at the 5% level taking into account the effect of serial correlation.

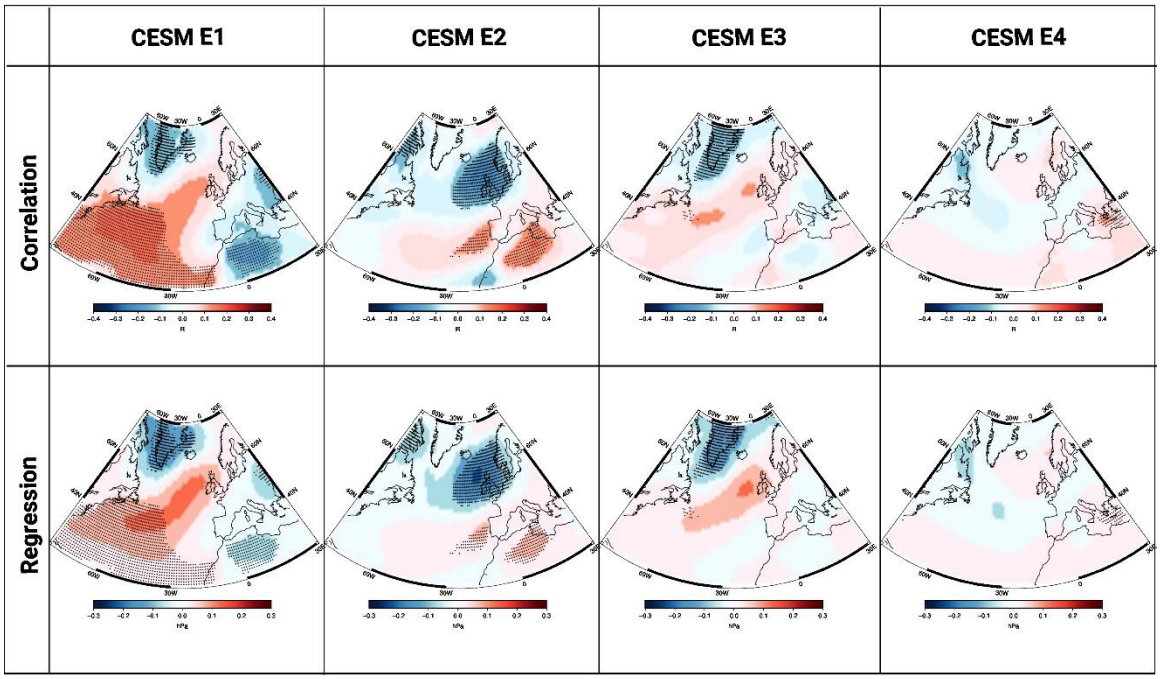


**Figure S9.** Spatial climatic response patterns of the North Atlantic SLP due to TSI changes during the summer, as calculated with linear methods for the period 850–1849 AD and for decadal time scales. The spatial correlation between TSI and the NA SLP is given in the first row. The second row contains the results of the regression of the TSI anomalies to the NA SLP. In the case of the linear regression, the units refer to changes of 1 standard deviation. The results are given for the realizations E1, E2, E3 and E4 of the CESM model in the first, second, third and fourth column, respectively. The hatched areas indicate statistical significance at the 5% level taking into account the effect of serial correlation.

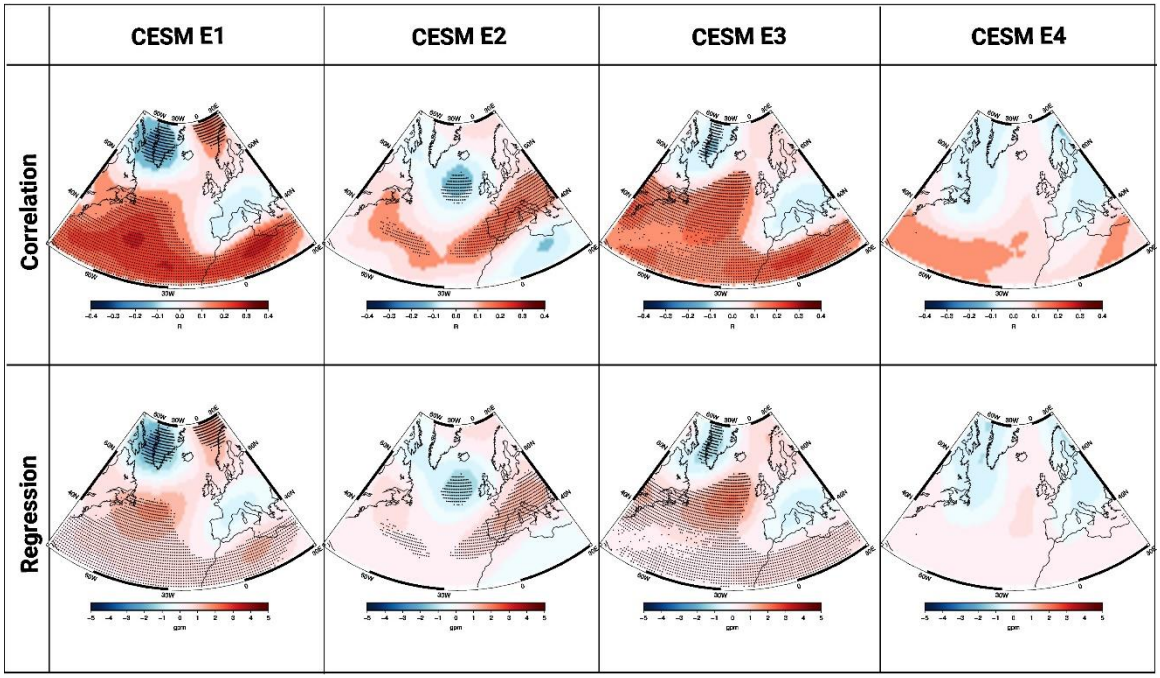


**Figure S10.** Spatial climatic response patterns of the North Atlantic geo500 due to TSI changes during the summer, as calculated with linear methods for the period 850–1849 AD and for decadal time scales. The spatial correlation between TSI and the NA geo500 is given in the first row. The second row

contains the results of the regression of the TSI anomalies to the NA geo500. In the case of the linear regression, the units refer to changes of 1 standard deviation. The results are given for the realizations E1, E2, E3 and E4 of the CESM model in the first, second, third and fourth column, respectively. The hatched areas indicate statistical significance at the 5% level taking into account the effect of serial correlation.

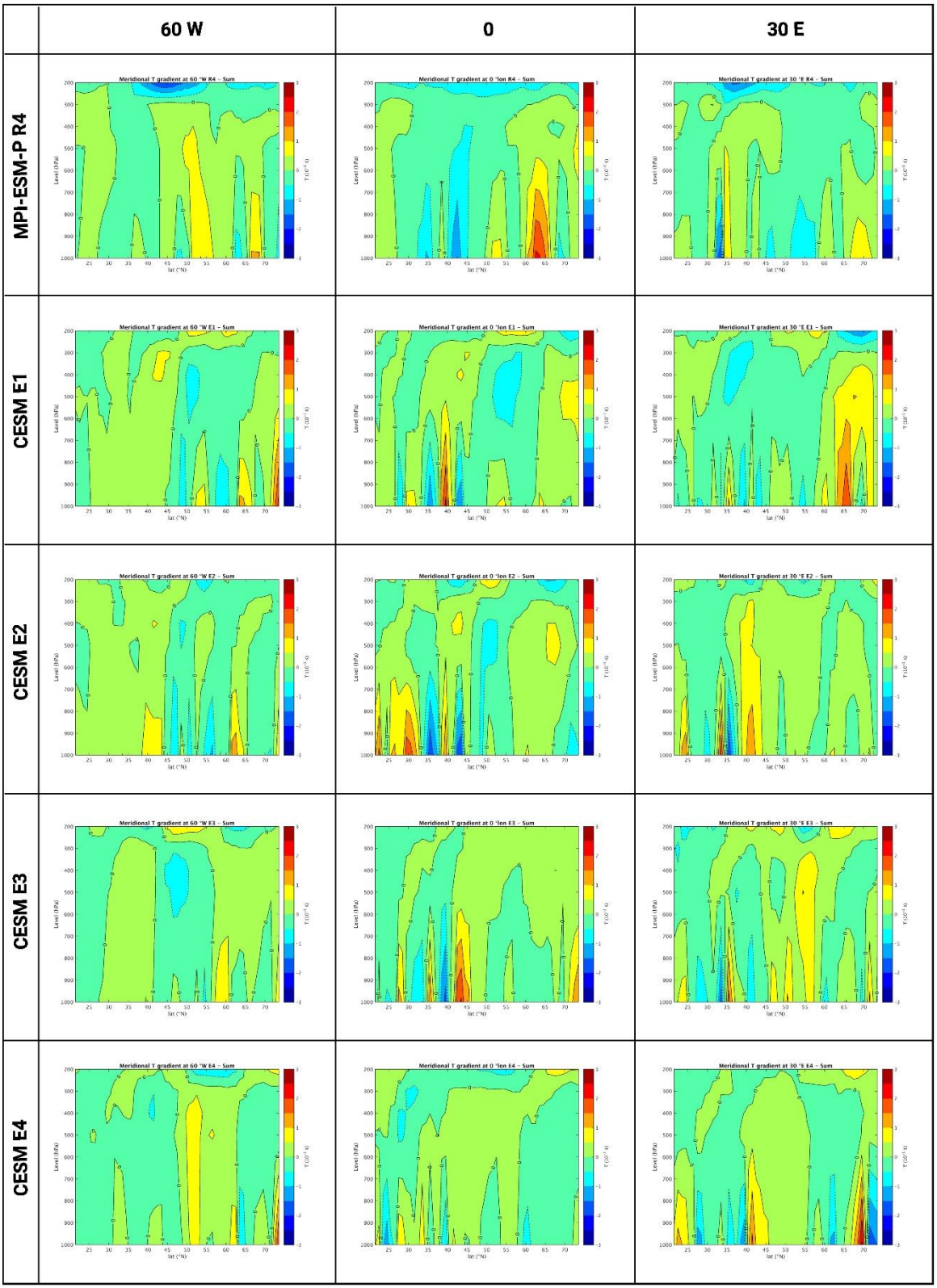


**Figure S11.** Meridional TA gradient for different atmospheric pressure levels, for 60° W (column 1), 0° (column 2) and 30° E (column 3). The results are given for the realization R4 of the MPI-ESM model and for the ensemble members E1, E2, E3 and E4 of the CESM model in the first, second, third and fourth row, respectively.

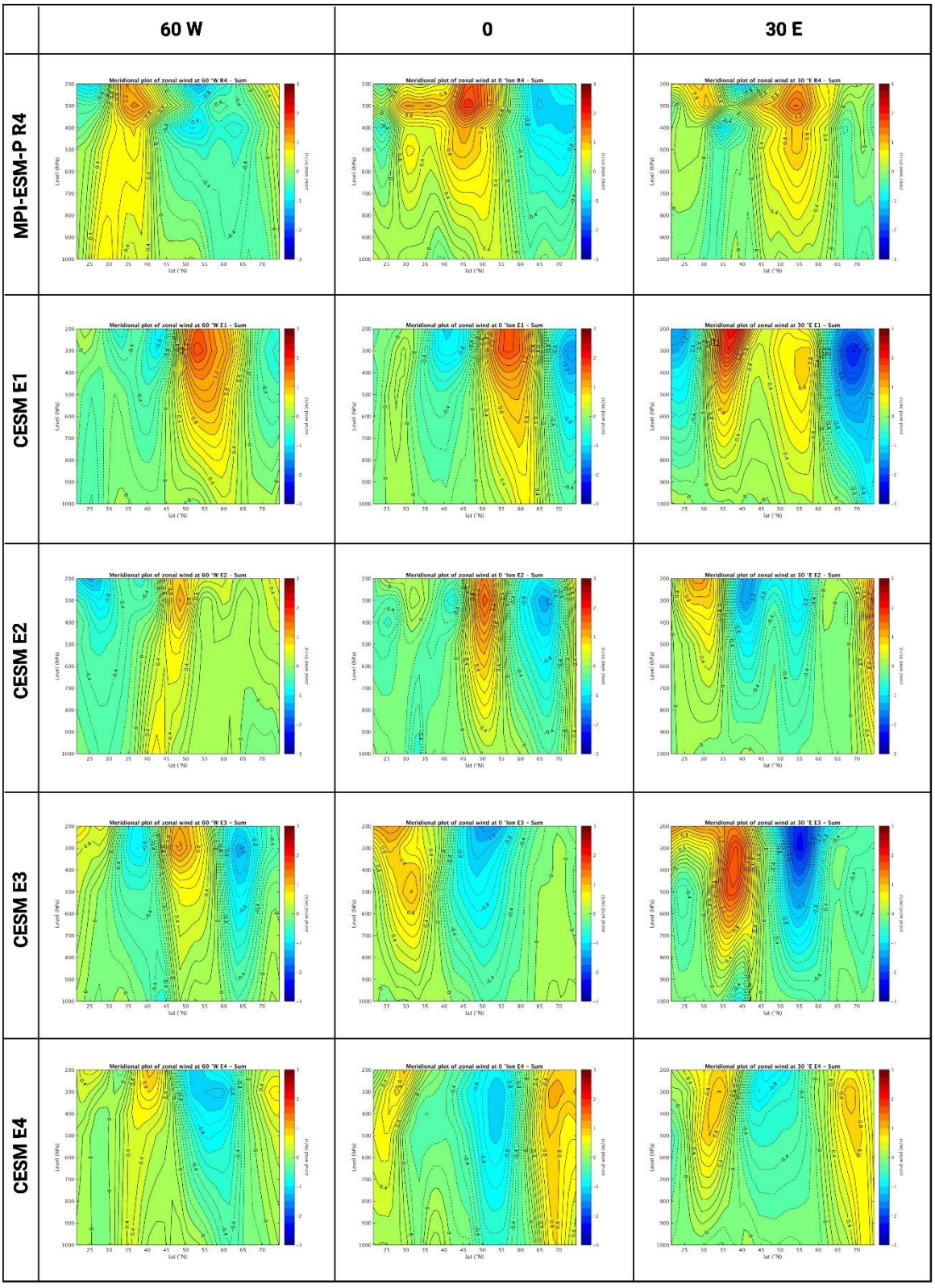


**Figure S12.** Meridional plot of U for different atmospheric pressure levels, for 60° W (column 1), 0° (column 2) and 30° E (column 3). The results are given for the realization R4 of the MPI-ESM model and for the ensemble members E1, E2, E3 and E4 of the CESM model in the first, second, third and fourth row, respectively.

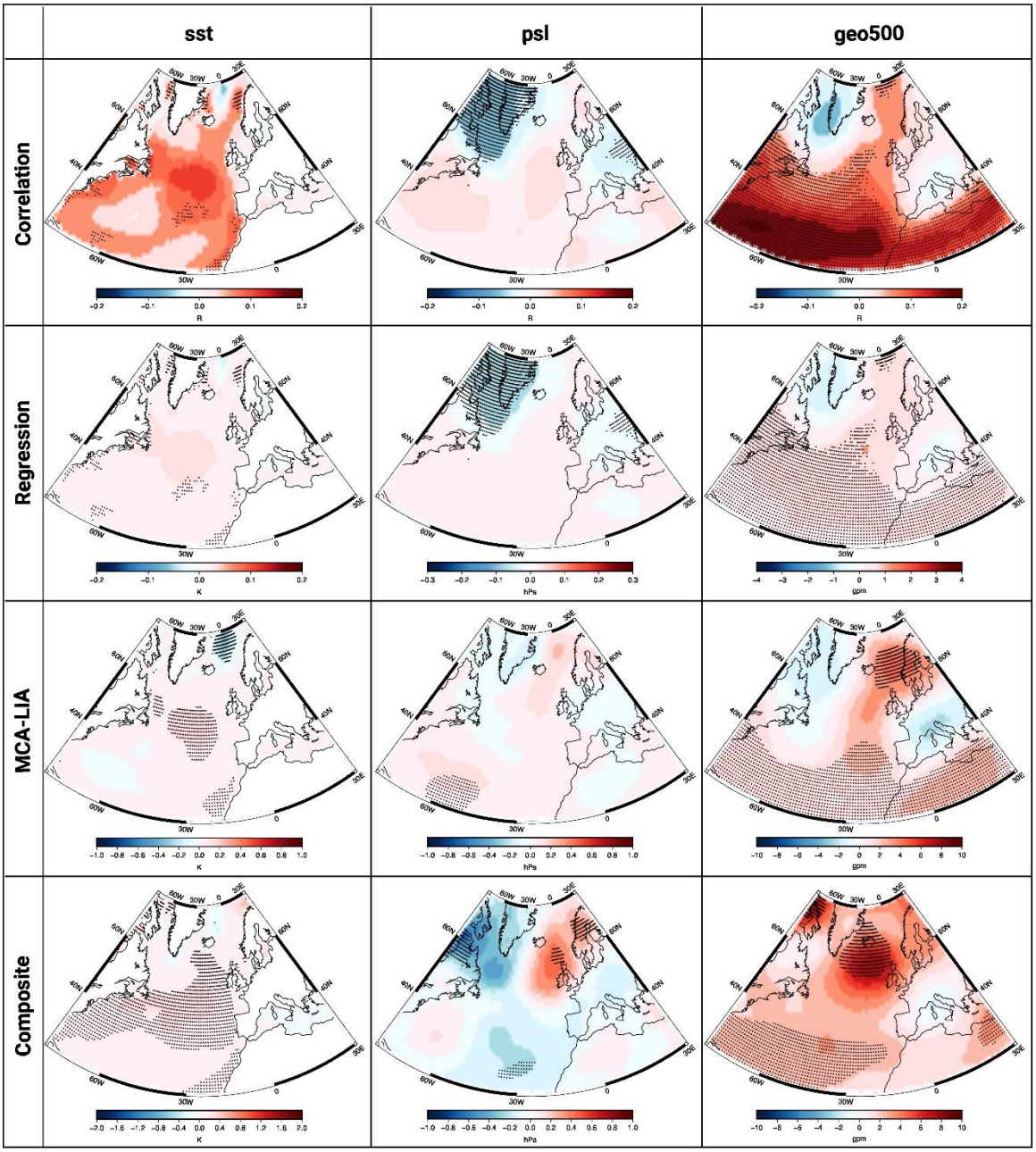


**Figure S13.** Spatial climatic response patterns to TSI of the North Atlantic summer SSTs (first column), SLP (second column) and geo500 (third column) as calculated with four different methods. The results are given for the CESM ensemble mean. The hatched areas indicate statistical significance at the 5% level taking into account the effect of serial correlation. In the case of the linear regression, the units refer to changes of 1 TSI standard deviation.

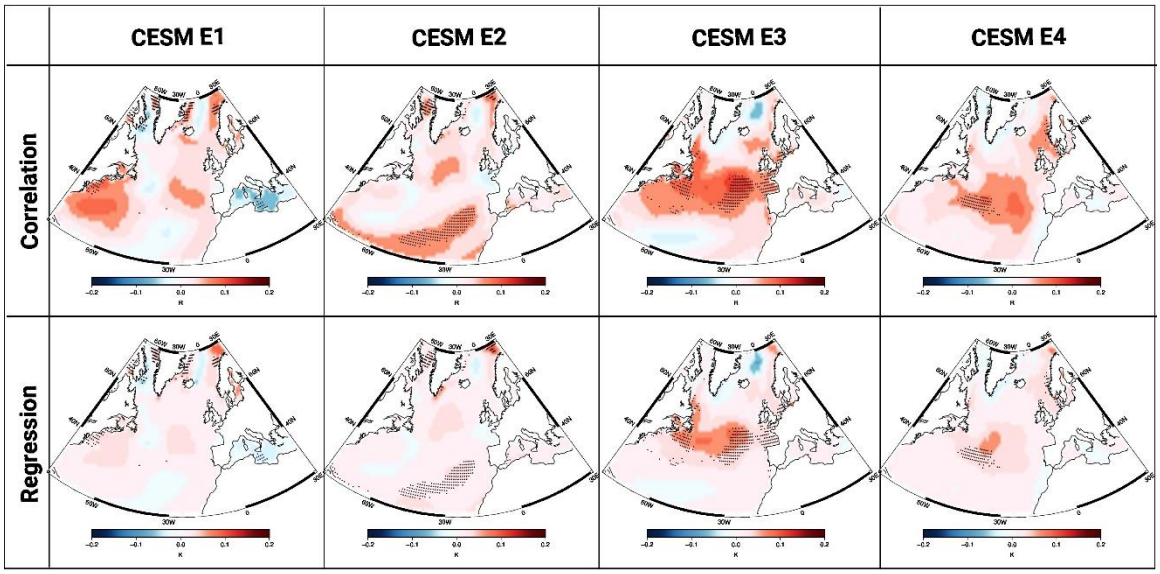


**Figure S14.** Spatial climatic lagged response patterns of the North Atlantic SSTs due to TSI changes during the summer, as calculated with linear methods for the period 850–1849 AD and for inter-annual time scales. TSI leads by 3 years. The spatial correlation between TSI and the NA SSTs is given in the first row. The second row contains the results of the regression of the TSI anomalies to the NA SSTs. In the case of the linear regression, the units refer to changes of 1 TSI standard deviation. The results are given for the realizations E1, E2, E3 and E4 of the CESM model in the first, second, third and fourth column, respectively. The hatched areas indicate statistical significance at the 5% level taking into account the effect of serial correlation.

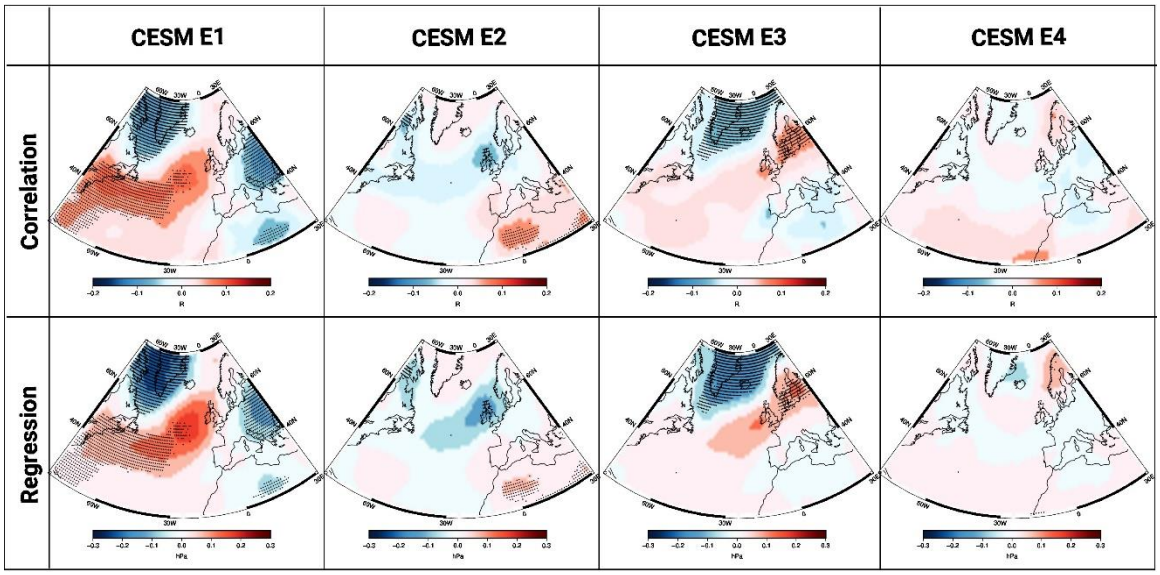


**Figure S15.** As in S14, but for SLP.

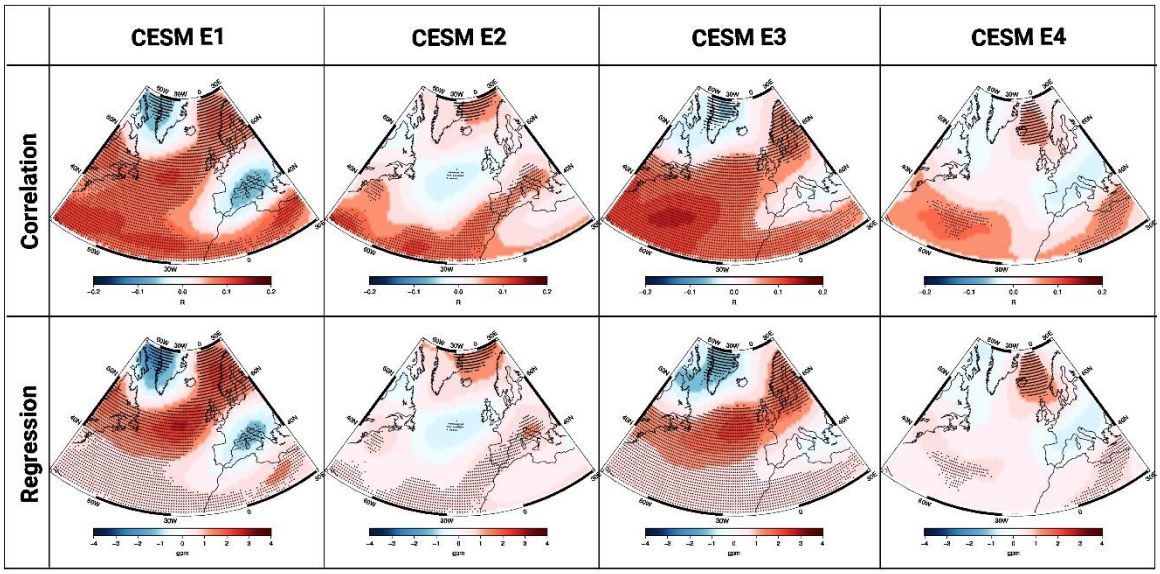


**Figure S16.** As in S15, but for geo500.